Pergamon

Geochimica et Cosmochimica Acta, Vol. 61, No. 7, pp. 1437-1446, 1997
Copyright © 1997 Elsevier Science Ltd
Printed in the USA. All rights reserved
0016-7037/97 $17.00 + .00

PII S0016-7037(97)00015-X

Association of cobalt and manganese in aquatic systems: Chemical and microscopic evidence

CHARLES-PHILIPPE LIENEMANN,[1] MARTIAL TAILLEFERT,[2] DIDIER PERRET,[1] and JEAN-FRANÇOIS GAILLARD[2,]*
[1]Institut de Chimie Minérale et Analytique, Universite de Lausanne, CH-1015 Lausanne, Switzerland
[2]Department of Civil Engineering, Northwestern University, Evanston, Illinois 60208-3109, USA

(*Received March* 25, 1996; *accepted in revised form January* 2, 1997)

Abstract—The distributions of cobalt and manganese in the water column of Paul Lake, a small meromictic lake located in the upper Michigan peninsula, follow remarkably similar patterns. At the oxycline, these elements show pronounced concentration gradients. In May 1994, Co and Mn increase from detection limits to 6 nM and 3 μM, respectively. The association between Co and Mn can be attributed to the sorption of cobalt to manganese hydrous oxides, and the redox-driven interconversion between dissolved Mn and particulate Mn-oxides species, which is often mediated by micro-organisms.

In this paper, we have used a multi-method approach to the study of Co:Mn association in an aquatic system. First, using equilibrium calculations, we discuss the chemical speciation of dissolved Co and Mn in the water column. Second, we present a Transmission Electron Microscopic (TEM) characterization of individual Mn-rich micro-particles. These particles were primarily observed at the oxic/anoxic transition. Micrographs confirm the biological origin of the hydrous manganese oxides. Analytical Electron Microscopy clearly establishes that Co and Fe are scavenged by micro-organisms bearing a Mn-oxide crust. Co:Mn ratios were determined on individual particles by Energy Dispersive Spectrometry (EDS). The comparison of the average Co:Mn ratio in particles to the one in solution shows that Co is enriched in the Mn-oxides overgrowths. High resolution TEM-EDS analyses of environmental particles proves to be a powerful tool to unveil chemical associations that are difficult to deduce from changes in the water chemistry. *Copyright © 1997 Elsevier Science Ltd*

1. INTRODUCTION

Cobalt is a transition metal of biological and economical importance. It is an essential oligo-element, playing an important role in the bio-methylation of heavy metals, e.g., Hg (Fergusson, 1990). At high concentration (>17 μM) Co is toxic to living organisms, but these concentrations are rarely, if ever, observed in the environment (Williams, 1971; Schrauzer, 1991). In pristine freshwater systems, it is usually present in trace amounts, around a few nano-molar (Forstner and Wittmann, 1979). Cobalt is also a metal of environmental interest since the radionuclide ^{60}Co is an activation product of radioactive wastes and has been identified as a priority contaminant (U.S. Department of Energy, 1994). Cobalt is released to the environment from the burning of fossil fuels and is consequently transported through the atmosphere. Soils, dust, and seawater have been recognized as important natural sources of Co and contributes to its global biogeochemical cycle (Schrauzer, 1991).

The geochemical behavior of Co in aquatic systems has often been related to the presence and oxidation of Mn (e.g., Spencer et al., 1972; Murray, 1975) and Fe (Balistrieri et al., 1992b). The oxidation of Mn(II) to Mn(III-IV) oxides, or MnO_x, is autocatalytic, and in natural systems it is also mediated by micro-organisms (Diem and Stumm, 1984; Nealson et al., 1988). Microbial catalysis has been observed at oxic/anoxic boundaries in marine systems (Emerson et al., 1982; Tebo, 1991) and in lakes (Chapnick et al., 1982; Gregory and Staley, 1982; Richardson et al., 1988; Tipping et al., 1985).

The chemical association of Co and Mn has been primarily inferred from the analysis of bulk water samples (e.g., Balistrieri et al., 1992b, 1994), because the direct determination of Co in environmental Mn-rich micro-particles has never been performed. Moreover, the speciation of trace elements like Co has been limited by collection artifacts and analytical difficulties. Membrane clogging, equilibrium shifts, differential sedimentation, and resuspension impede particle size fractionation schemes that use either filtration or centrifugation. These obstacles apply not only to the determination of trace concentrations of dissolved species, but also to the chemical analysis of micro-particles and colloids (Honeyman and Santschi, 1988, 1992; Buffle et al., 1992). The detection limit of conventional trace analysis techniques, e.g., graphite furnace atomic absorption, usually requires a pre-concentration step for the analysis of water samples. Furthermore, the direct inspection and analysis of environmental micro-particles, which have been recognized as potential trace element carriers, is still in its infancy (Leppard, 1992).

Consequently, the current understanding of the behavior of trace elements in the presence of particulate material relies on recent conceptual advances made in aquatic surface chemistry (Stumm, 1992). These concepts have been verified with laboratory experiments that have consistently used concentrations of dissolved elements and model particles which are orders of magnitude higher than those encountered in natural systems (Stumm, 1993). Their application to the speciation of metals in natural aquatic systems requires further detailed field studies and concurrent progresses in the analytical chemical speciation of trace elements.

In this research, we have investigated an alternative ap-

---

*Author to whom correspondence should be addressed (jf-gaillard @nwu.edu).

proach based on the analysis of water samples and individual micro-particles to demonstrate the unequivocal association of Co and Mn. This study was performed in a small meromictic lake (Paul Lake, MI) where the chemical signatures are intensified at the oxic/anoxic transition.

2. STUDY AREA

Paul Lake is located at UNDERC (University of Notre Dame Environmental Research Center), at the border of Wisconsin and the upper peninsula of Michigan, USA (Fig. 1). The center of the property is positioned at 46°13′N 89°32′E, with an altitude range between 500 and 520 m. UNDERC lies in Northern Highland Province, which is the southernmost extension of the Canadian Shield. This province is characterized primarily by Pre-Cambrian bedrocks capped by a thin layer of sedimentary rocks left by the Paleozoic seas. On top of this formation are glacial deposits left by the Woodfordian and Valderan substages of the Wisconsinian glaciers. These glacial deposits are young and the drainage system is poorly developed. The surface deposits are characteristic of glacial retreat, consisting of infertile, sandy, pitted glacial out-wash or boulder and clay morainic deposits. As a result of their composition, the soils have a reduced capacity for cation exchange, leaving them very susceptible to acidification. Many of the lakes in this region are kettle lakes, others originate from irregular depressions in the ground moraine or were scoured out of the bedrock as the glaciers passed.

Paul Lake has a surface area of 1 ha, a mean depth of 6 m, and a maximum depth of 13 m (Fig. 1). All the water entering Paul Lake comes from atmospheric deposition and groundwater seepage. Paul Lake generally remains stratified year-long because of a biogenic meromixis (Carpenter and Kitchell, 1993) and has been classified mesotrophic (St. Amand, 1990). The concentration of soluble reactive phosphorus remains low in surface waters year-long, but nutrient regeneration at the oxic/anoxic transition promotes phytoplanktonic blooms just above this interface (Carpenter and Kitchell, 1993).

3. METHODS

The water column chemistry of Paul Lake was investigated in May 1994 (water sampling) and July–August 1995 (water and particle sampling). The chemical distribution of the dissolved species, major and trace elements, as well as the elemental analysis of the micro-particles formed at the oxic/anoxic transition, was determined. We present here the results relevant to the partitioning of Co and Mn between the dissolved and particulate phases, as obtained by two complementary analytical tools: ICP-MS and TEM-EDS.

3.1. Water Sampling and Analysis

The physical and chemical characteristics of Paul Lake were established using a portable CTD-pH-O_2 probe (Scout, Hydrolab). The response of the O_2-probe was standardized by concurrent Winkler titrations. Water samples were collected every 50 cm by peristaltic pumping using a portable, battery operated, pump (Cole Parmer) with acid-cleaned Tygon^R tubing. The samples were retrieved in line, i.e., without contact to the atmosphere, using pre-cleaned syringes made of a polypropylene barrel and polyethylene plunger (HSW). The waters were subsequently filtered through acid-cleaned 0.45 μm Acrodisc LC-PVDF Gelman filters. The first fractions of filtrate were discarded, and subsequent aliquots were preserved for the analysis of trace elements in acid-cleaned polypropylene tubes (Falcon) and for the analysis of major and minor species in cleaned polypropylene bottles (Nalgene). All the sampling equipment and the containers were cleaned with HNO_3 Trace Metal Grade (Fisher) and Millipore Milli-Q water.

At UNDERC, the determination of ΣH_2S was performed on 50 mL aliquots, preserved at pH = 10 using NaOH. Within an hour, the samples were titrated with $HgCl_2$ using an Ag/Ag_2S electrode and a double junction reference electrode. A computerized titration scheme was developed from the manual method of Boulègue et al. (1979), and the equivalence point was determined by means of a Gran function (Dyrssen and Wedborg, 1986). The concentration of dissolved ferrous iron, $Fe(II)_d$, was determined by colorimetry using ferrozine (Stookey, 1970), while total iron, Fe_T, was determined similarly after reacting unfiltered samples with hydroxylamine hydrochloride. The positive interference of Fe^{3+} on the Fe^{2+}/ferrozine colorimetric determination (Siffert, 1989) was checked with standard Fe^{3+} solutions in the range 10^{-6} to 2×10^{-4} M, but was found to be negligible for the concentrations of $Fe(III)_p$ found in Paul Lake ($[Fe(III)_p] = 2.5 \times 10^{-5}$ M produces a colorimetric signal equivalent to 10^{-7} M Fe^{2+}). The turbidity of the bulk water samples was determined using a Hach 2100 A turbidimeter.

In the laboratory, Fe_T recovery was checked using Atomic Absorption Spectrometry (AAS, Varian SpectrAA-20). Particulate iron,

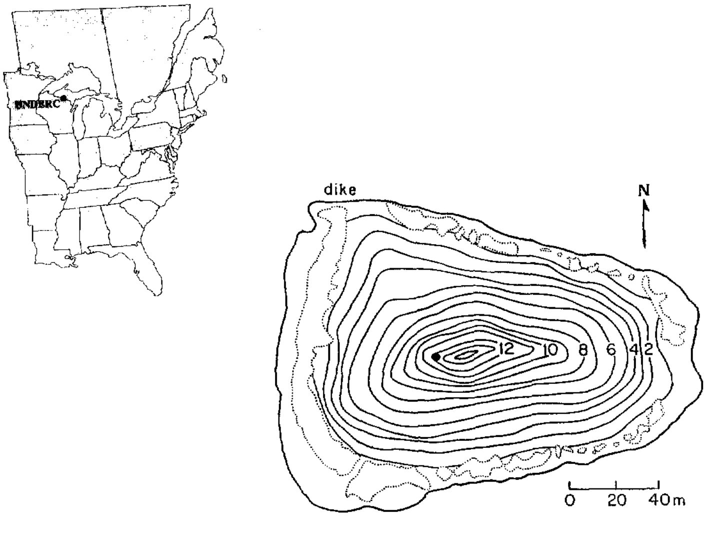

Fig. 1. Location and bathymetric chart of Paul Lake, UNDERC, Michigan, USA. The filled circle indicate the sampling location.

Fe_p, was determined by difference: $Fe_p = Fe_T - Fe(II)_d$. Dissolved manganese was determined either as Mn^{2+}, by capillary electrophoresis (CE, Waters), or as total dissolved manganese (AAS and ICP-MS). The water samples were analyzed for trace elements by Inductively Coupled Plasma Mass Spectrometry ICP-MS (VG-Plasma-Quad2-STE) on the acidified aliquots. Indium, terbium, and yttrium were used as internal standards. Quality control was performed using 1 ppb standards and the National Research Council Canada river water standard SLRS-2. The preparation of the samples, standards, and reference solution was conducted in a clean laboratory in order to minimize contamination. The detection limit, reported within a confidence interval of 3σ, was 0.3 nM for Co.

3.2. Micro-Particles: Sampling and Analysis

The bulk water samples were collected by peristaltic pumping and were retrieved, in line, using 50 mL syringes as described before. The syringes were immediately sealed, transferred to a N_2-purged glove-bag (model X27-27, I^2R), and brought to the laboratory. TEM grids (200 mesh, Cu, carbon-coated and collodion-covered, SPI Supplies) were placed at the bottom of centrifuge tubes (Nalgene). Under N_2 atmosphere, an aliquot of the bulk water sample was transferred to centrifuge tubes (30 mL) which were tightly sealed. The volume of aliquot used was determined from turbidity measurements to insure an appropriate micro-particle coverage of the grid. The tubes were spun under nitrogen atmosphere, within 30 min after retrieval from the field, for 14 h at 6000 rpm using a swing-out rotor in order to obtain whole mount specimens. After centrifugation, the tubes were transferred to a glove-bag and the supernatant was carefully withdrawn, by slow nonturbulent pipetting. The TEM grids were then protected with a thin film of hydrophilic resin (Nanoplast FB101; Plano). Previous laboratory tests showed that, under these conditions, Fe^{2+} is not oxidized into $Fe(III)_p$. More details about this sampling procedure are presented in Perret et al. (1991).

The grids were first observed on a Jeol 100C TEM (University of Notre Dame, Indiana, USA) to verify the optimal deposition and lay-out of the micro-particles. TEM identifications were then performed on a medium-resolution TEM Zeiss EM10 (Centre de Microscopie Electronique, University of Lausanne), while elemental microanalyses were performed on a High Resolution Electron Microscope (HREM, Hitachi HF-2000 FEG, Centre Interdépartemental de Microscopie Electronique, EPFL, Lausanne). This instrument is equipped with a narrow probe (ca. 2 nm in diameter) that provides X-ray spectrometry (EDS) with a high lateral definition. The beam sampling depth was estimated to equal the thickness of the analyzed particles under the conditions of operation. Spectra were acquired and analyzed using the Noran Voyager software running on a Sun SparkStation IPX. For the optimal determination of elements present in low concentration, analyses were performed under the following conditions: acquisition time: 80–300 sec spot size: (3–5) nm^2 (depending on particle size), beam current 10^9 e^-/nm^2, magnification: $7 \times 10^4 - 5 \times 10^5$ ×, EDS detector: Ge with a Norvar window.

Spectral deconvolutions were accomplished by performing multiple Gaussian fitting of the spectra using theoretical energies corresponding to (1) Mn K_α (5.894 keV), (2) Fe K_α (6.398 keV) plus Mn K_β (6.489 keV), and (3) Co K_α (6.924 keV) plus Fe K_β (7.057 keV). For each peak, the width obtained by adjustment was consistently ca. 145 eV, which is in perfect agreement with the resolution of the detector determined on Mn-standard material (146 eV). Quantitative standardless analyses (Reed, 1993) were effected using fitted peak heights and theoretical intensities of the K_α transitions of Mn, Fe, and Co.

4. RESULTS AND DISCUSSION

In this section, we present first the water column chemistry, emphasizing the chemical gradients observed at the oxic/anoxic transition, and the results of thermodynamic calculations providing some insights into the chemical speciation. Then, we proceed with a short description of the particulate material, as observed by TEM, while focusing on the morphology and elemental composition of Mn-rich micro-particles.

4.1. Characterizing the Oxic/Anoxic Transition

The water column profiles of temperature, O_2, pH, $SO_4^=$, and ΣH_2S, observed in May 1994, are shown in Fig. 2. The distribution of the concentrations of dissolved cobalt (Co_d) and dissolved manganese (Mn_d), observed in May 1994 and July–August 1995, are presented together with the May 1994 profiles of dissolved iron (Fe_d) and particulate iron (Fe_p) in Fig. 3. The concentrations of particulate Mn were below our detection limits, since the differences between Mn_T and Mn_d were always small. All these profiles demonstrate that large gradients of concentration occur in the water column as a result of the oxic/anoxic transition.

In May 1994, the temperature profile clearly establishes the extent of the thermal stratification. The oxycline spans over depths ranging from 4.5 to 6 m. The profile of dissolved O_2 concentration shows a pronounced maximum above the chemocline as a result of photosynthetic activity. The variations of pH reflect the major biogeochemical processes taking place in the water column: above the oxycline, the photosynthetic activity leads to an increase in pH, whereas the utilization of O_2, either for the oxidation of biogenic organic matter or reduced species (e.g., Mn^{2+} and Fe^{2+}), results in a pH decrease. The driving reactions, at the oxycline, can be summarized as follows:

$$CH_2O + O_2 \rightarrow CO_2 + H_2O \quad (1)$$

$$4\,Fe^{2+} + O_2 + 10\,H_2O \rightarrow 4\,Fe(OH)_{3(s)} + 8H^+ \quad (2)$$

$$2\,H_2O + 2\,Mn^{2+} + O_2 \rightarrow 2\,MnO_2 + 4H^+ \quad (3)$$

where CH_2O stands for the metabolizable fraction of natural organic matter. At depth, the pH stabilizes around 6.3, where the buffering capacity of the carbonate system ($H_2CO_3^*/HCO_3^-$) is maximum. This demonstrates that, in the anaerobic region, the pH is controlled by inorganic carbon species.

The concentration of sulfate decreases below the oxycline from 12 μM to below the detection limit (<0.2 μM), and total sulfides (ΣH_2S), produced by sulfate reducing bacteria and the anaerobic decomposition of organic matter, become detectable at a depth of 7 m and reach 8 μM in deep waters. The concentration of dissolved Fe^{2+} increases sharply at 7 m to reach 75 μM at depth, whereas the concentration of Fe_p shows a pronounced peak ($Fe_p = 25$ μM) at a depth of 6 m, the end of the oxic/anoxic transition zone. On the other hand, the concentrations of dissolved Mn and Co increase sharply across the oxic/anoxic transition, from 5 to 5.5 m depth. The concentration of Co rises from detection limit, when O_2 is still present, to 6.8 nM and 12 nM, respectively, for May 1994 and July–August 1995. Similarly Mn increases from detection limit to, respectively, 3 μM and 4 μM. Analogous profiles for these major and minor species, obtained from the water column of various dimictic or meromictic lakes, have been reported in the literature (i.e., Balistrieri et al., 1992a,b, 1994; Michard et al., 1994; Viollier et al., 1995). The key features of our study are: (1) The maximum concentration of Fe_p occurs in the suboxic region where oxygen is almost entirely depleted, which shows that the interplay between transport and reaction determines the location of the particulate iron peak. (2) From the inspection of the concentration profiles of Co, Mn, and Fe, the speciation

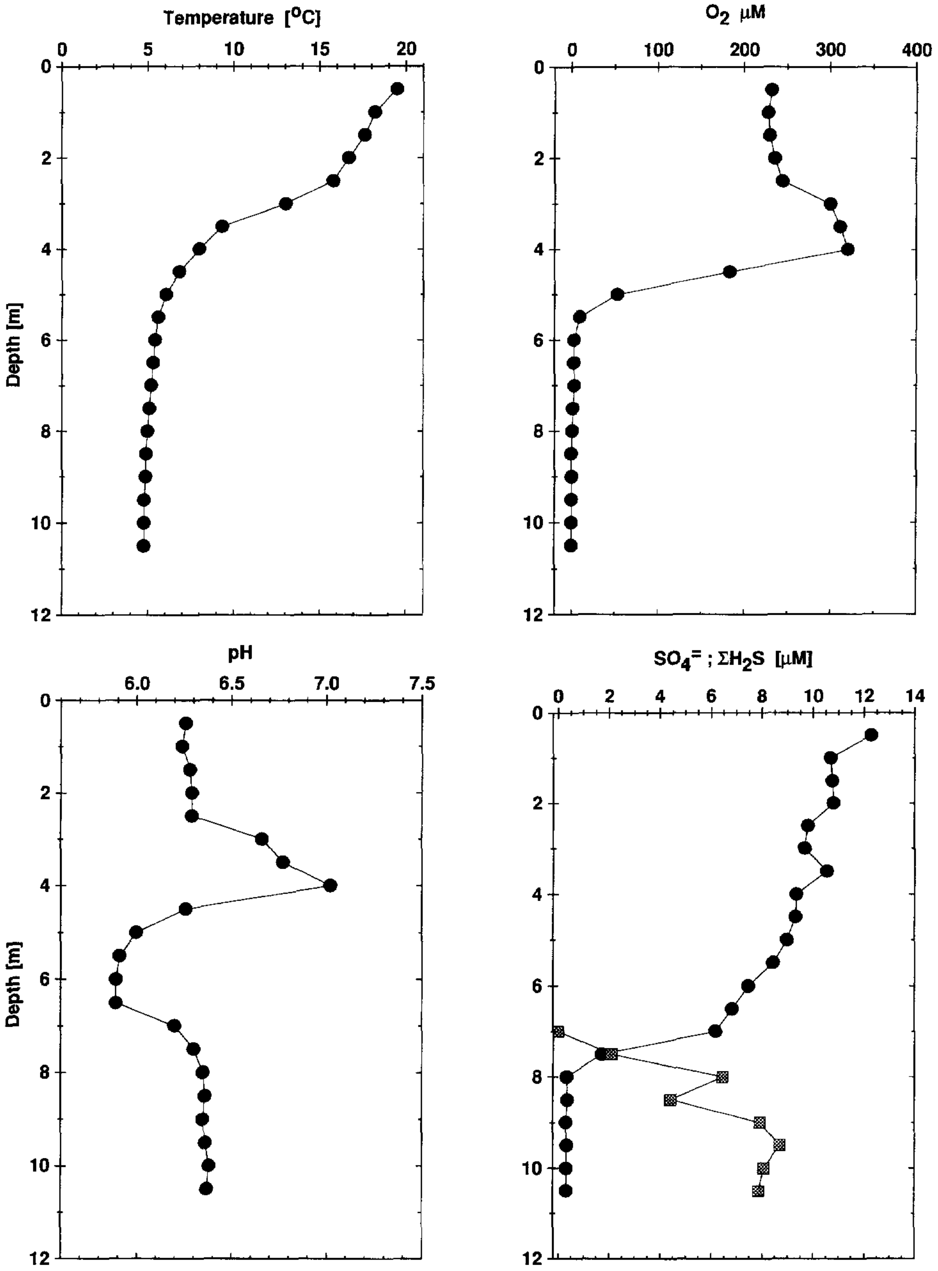

Fig. 2. Depth profiles of temperature, dissolved oxygen, pH, and dissolved sulfur species: ΣH_2S (shaded squares), $SO_4^=$, in the water column of Paul Lake (May 1994).

of Co appears mainly linked to Mn, because the well developed peak of particulate iron does not influence significantly Co concentrations. If Fe_p is involved in the scavenging of Co, as reported by Balistrieri et al. (1992b), it must be to a lesser and not discernible extent.

4.2. Chemical Speciation from Solution Chemistry

The chemical speciation of Paul Lake's water column was computed using PHREEQC (Parkhurst, 1995) and the complete set of water analyses (May 1994) to assess the likelihood of the presence of mineral phases (i.e., oxides or sulfides) and the distribution of dissolved species. The thermodynamic database was extended to include cobalt and sulfide complexes were updated using recent compilations (Dyrssen and Kremling, 1990; Balistrieri et al., 1992b). These calculations provide, however, only a qualitative framework for interpreting solution chemistry, since true and complete equilibria are rarely attained in low temperature aquatic environments. Moreover, we have presently little information on the complexing nature of the dissolved organic matter and equilibrium constants for metal sulfide complexes remain questionable. Nonetheless, the major chemical species that should prevail can be delineated. In the oxic mixolimnion, dissolved Co remains primarily under its free hydrated form ($Co[H_2O]_6^{2+}$), whereas in the anoxic bottom waters it seems to be primarily present as a sulfide complex (CoS^0). In the oxic/anoxic transition zone when

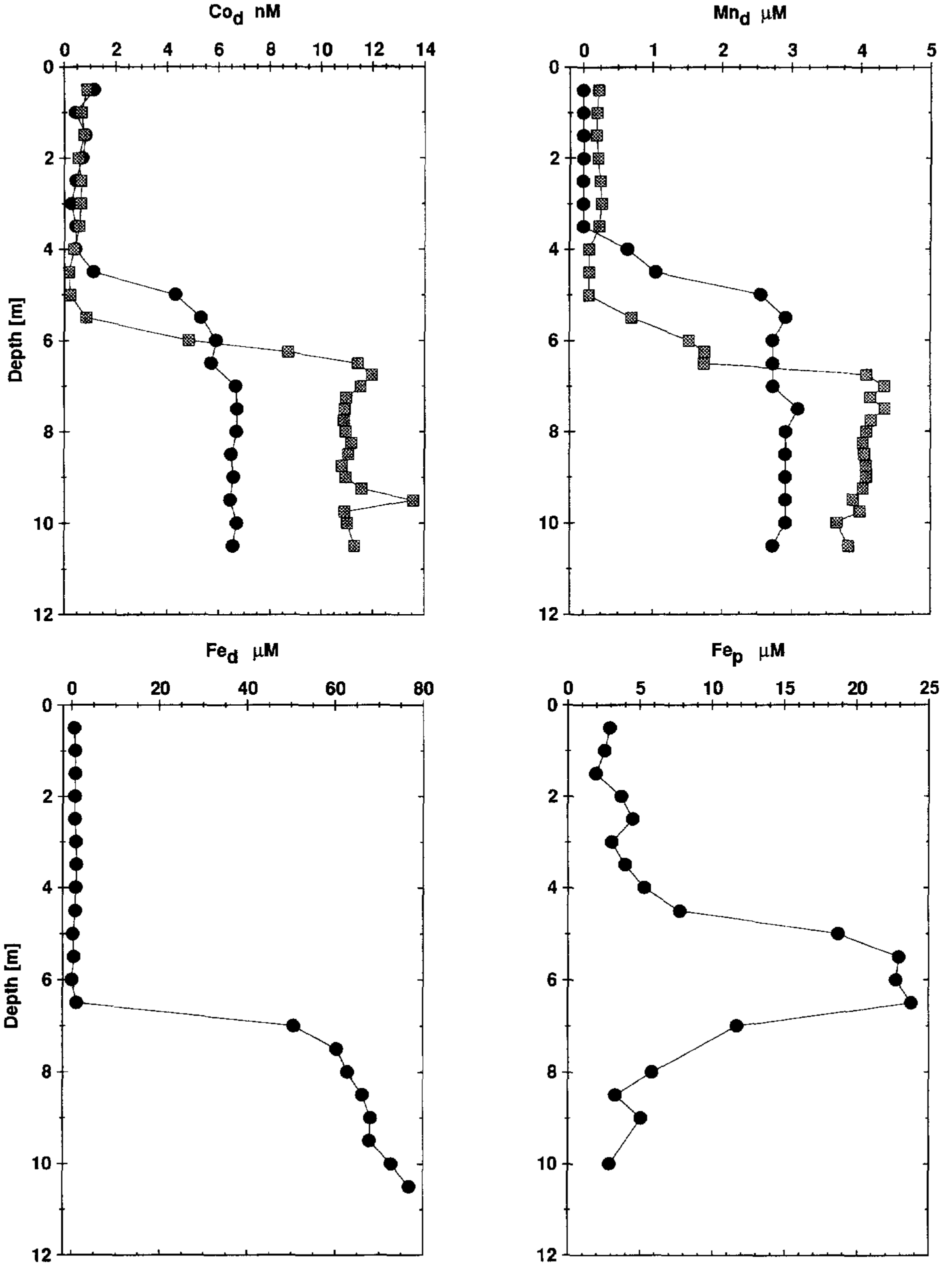

Fig. 3. Concentration profiles of dissolved cobalt (Co$_d$), manganese (Mn$_d$), and iron (Fe$_d$), and of particulate iron (Fe$_p$) in the water column of Paul Lake. Filled circles: May 1994, shaded squares: July–August 1995. Note that during the summer 1995 the oxycline was 1.5 m below that of May 1994.

oxygen is still present, dissolved manganese, measured as Mn^{2+} by CE, is supersaturated with respect to manganese oxides, i.e., manganite (MnOOH) and the allotropic forms of pyrolusite (MnO_2), whereas in the anoxic zone the predominant species is free Mn^{2+}. With respect to Fe, the only potentially stable mineral phase predicted by thermodynamic calculations is amorphous iron sulphide (FeS_p) which reaches saturation: $\Omega_{FeS} = 1.175$, where $\Omega_{FeS} = IAP/K_S$ in bottom waters. In oxic waters, dissolved iron remains below detection limits. At depth, the presence of small amounts of ΣH_2S may contribute to the reductive dissolution of the hydrous oxides of Mn and Fe formed in the oxic/anoxic transition (Burdige and Nealson, 1986; DeVitre et al., 1988).

4.3. Electron Microscopy

TEM investigations were carried out on four different grids for each depth. A two step approach was undertaken: (1) Observation of the different grids, reflecting the microscopic particulate material present in the water column, by conventional TEM. (2) Analysis of the micro-particles collected between 4 and 9 m by Energy Dispersive Spectrometry (TEM-EDS), in order to determine their elemental composition along the water column.

4.3.1. General Trends

One finds a great diversity of particles in the entire water column. The apparent size distribution ranges from a few

Fig. 4. Transmission electron micrograph of particles collected in the suboxic zone of Paul Lake water column. The black spherical micro-particles are bacteria covered by an electron dense material which is Mn-rich. The algae, shaped like tennis rackets, are chrysophytes of the genus *Synura spinosa* (bar = 2 μm).

nm to hundreds of μm. We observed predominantly organic fibrils, mixed aggregates of mineral and organic compounds, electron dense mineral particles, various diatoms, but rarely clay-like material. In the 5–5.5 m suboxic layer, numerous bacteria covered with electron dense inorganic deposits were encountered (Figs. 4 and 5a). TEM-EDS analyses revealed that these micro-particles are Mn-rich (Fig. 5b). Although these bacteria have not been identified yet, their morphology and the characteristics of their Mn-rich crust significantly differs from the *Metallogenium*-like particles (Schmidt, 1979) which systematically appear as dendritic entities, or from strains of *Siderocapsae* and *Leptothrix* (Ghiorse, 1984) exhibiting larger sizes and ellipsoidal shapes.

Although the bulk water concentration of Fe_p shows a pronounced peak centered at 6 m, almost all TEM-EDS measurements show the presence of Fe in particles along the entire water column, with the exception that their count is much higher at 6 m. Manganese, however, was clearly identified on EDS spectra of well distinct micro-particles exclusively localized at depth around 5 m, as illustrated on Fig. 5a. This can be attributed to a specific nucleation and growth of manganese hydrous oxides at the surface of some microorganisms, when suitable chemical conditions prevail as suggested by our previous calculations (see section 4.2). It is worthy to note that, even if the set of individual particles analyzed by EDS is relatively limited (n = 250 particles, ca. 30 particles at each sampling depth), measurements by TEM-EDS are able to evidence Mn-rich particulate material. The failure to observe Mn-rich particles at depths below 5.5 m is probably due to the negligible mass concentration of that species.

4.3.2. Analytical Electron Microscopy of Mn-Rich Particles

As mentioned earlier, we may infer, from the water chemistry data, that Co and Mn are intimately associated. Consequently, we focused our attention on a more detailed description of the elemental composition of these Mn-rich particles.

The spectrum presented in Fig. 5b shows interesting features in the 5.5–7.5 keV region. A spectral deconvolution allowed us to clearly demonstrate that Co and Fe were associated with the Mn-rich bacterial overgrowth (Fig. 6). In the spectral deconvolution presented, the only parameter fitted is the height of the peak. Although the signal to noise ratio is relatively low in the region of the Co (K_α) plus Fe (K_β) peak, it is possible to clearly identify Co. The majority of the spectra acquired on Mn-rich particles show a contribution from Co, with varying contributions from Fe.

4.4. Co:Mn and Fe:Mn Associations

As the concentrations of Co_p and Mn_p, determined by difference between total and dissolved fractions, are below detection limits, it becomes difficult to determine from concentration profiles the molar ratio of Co to Mn expected in the particulate phase. However, if we hypothesize that Co is scavenged uniquely by hydrous manganese oxides, and that these two elements are released concomitantly and completely during the reductive dissolution of these oxides at depth, a Co:Mn ratio can be inferred from the water data. A regression analysis between Co_d and Mn_d (Fig. 7) gives a molar Co:Mn ratio of $(2.6 \pm 0.02)10^{-3}$.

On the other hand, Co:Mn ratios of the Mn-rich overgrowth can be estimated, for each particle analyzed, using a standardless analysis of the TEM-EDS spectra. For the entire set of analyses, we obtained a Co to Mn ratio an order of magnitude higher, Co:Mn = $(2.0 \pm 0.7)10^{-2}$ ($n = 9$). In all the selected spectra the EDS signals for Co were four to six times higher than the 3σ detection limit. Similar estimates for the abundance of Fe in these Mn-rich particles led to Fe:Mn = 0.33 ± 0.29 ($n = 13$).

The Co:Mn ratio of the micro-particles is relatively close to the average value of Co:Mn in crustal rocks (2.6×10^{-2}) and the one observed in marine oxic waters (2.5×10^{-2}) (Whitfield and Turner, 1987). This ratio is, however, 1 order of magnitude larger than the one determined from the water data. This difference indicates that Co is significantly enriched in these Mn-rich micro-bioparticles compared to the solution. This is not a new finding, since manganese oxides have been used to concentrate Co (Fukai, 1968), but we present here direct evidence of this phenomenon at the level of individual particles present in an aquatic system.

The specific sorption of Co by manganese oxides has been documented in numerous laboratory and field studies (e.g., Spencer et al., 1972; Murray, 1975). Using X-Ray Photoelectron Spectroscopy (XPS), Crowther et al. (1983) have suggested that Co(II) is oxidized to Co(III). Recent EXAFS investigations of the crystal structure of γ-MnO_2, which certainly is the closest known model of the hydrous oxide formed

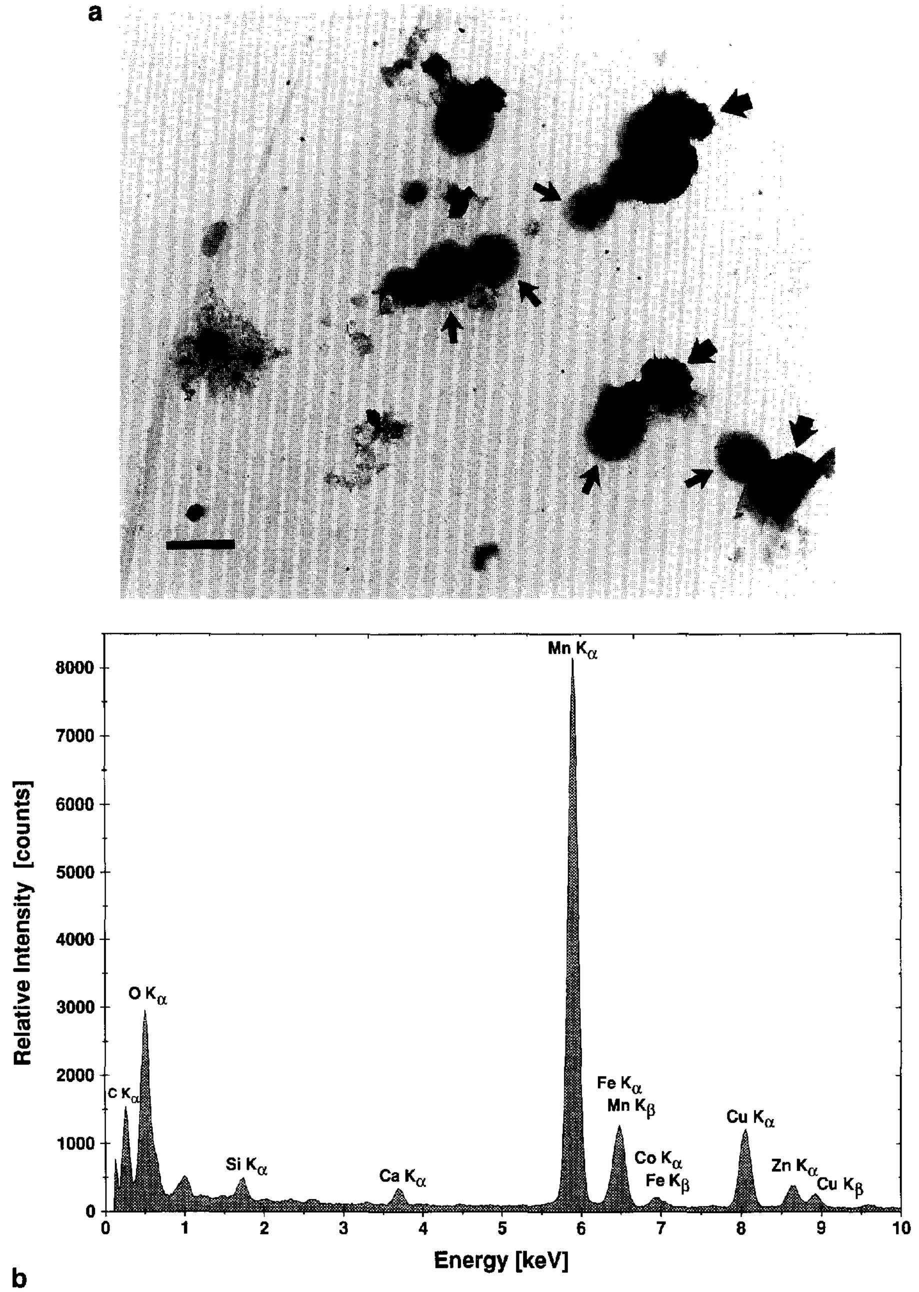

Fig. 5. (a) Close up micrograph showing the pool of bacteria present in high number concentration at 5 m depth. Some are covered with Mn-rich material (large arrow), whereas others (small arrow) show little evidence of Mn overgrowth (bar = 1 μm). (b) EDS spectrum of a Mn bearing bacteria. The Cu and Zn peaks originate from the TEM supporting grid.

at the surface of bacterial walls, have shown that it consists of assemblages of tunnels presenting numerous defects (Godart et al., 1992). In this environment, the Co^{2+} ion could be oxidized to Co^{3+} (Manceau et al., 1992), a d^6 ion able to exhibit octahedral coordination and having an ionic radius almost identical to Mn^{4+}. Unfortunately, we do not have, at present, any information about the valence states of Co nor Mn in these bacterial crusts, at the individual particle level. This information could be obtained by careful Electron Energy Loss Spectrometry (EELS) analysis of the Mn-rich particles. A recent study has shown that Mn(II) is directly oxidized to Mn(IV) by bacterial spores (Mandernack et al., 1995). This study does not provide any definitive conclusion on Co enrichment due to the selective sorption and oxidation of Co by manganese oxides, it only demonstrates their association on a per particle basis. One may also envision that biological pathways may be responsible for Co biomagnification and oxidation (Tebo et al., 1984; Lee and Tebo, 1994).

These results can be compared to recent estimates of Co:Mn ratios observed in anoxic waters of other lakes. In the case of Hall Lake (Balistrieri et al., 1994), a meromictic lake in Washington, this ratio was approximately 8.75 $\times 10^{-4}$, whereas for the hypolimnion of Lake Sammamish (Balistrieri et al., 1992b), it was 1.12×10^{-4}. For Aydat

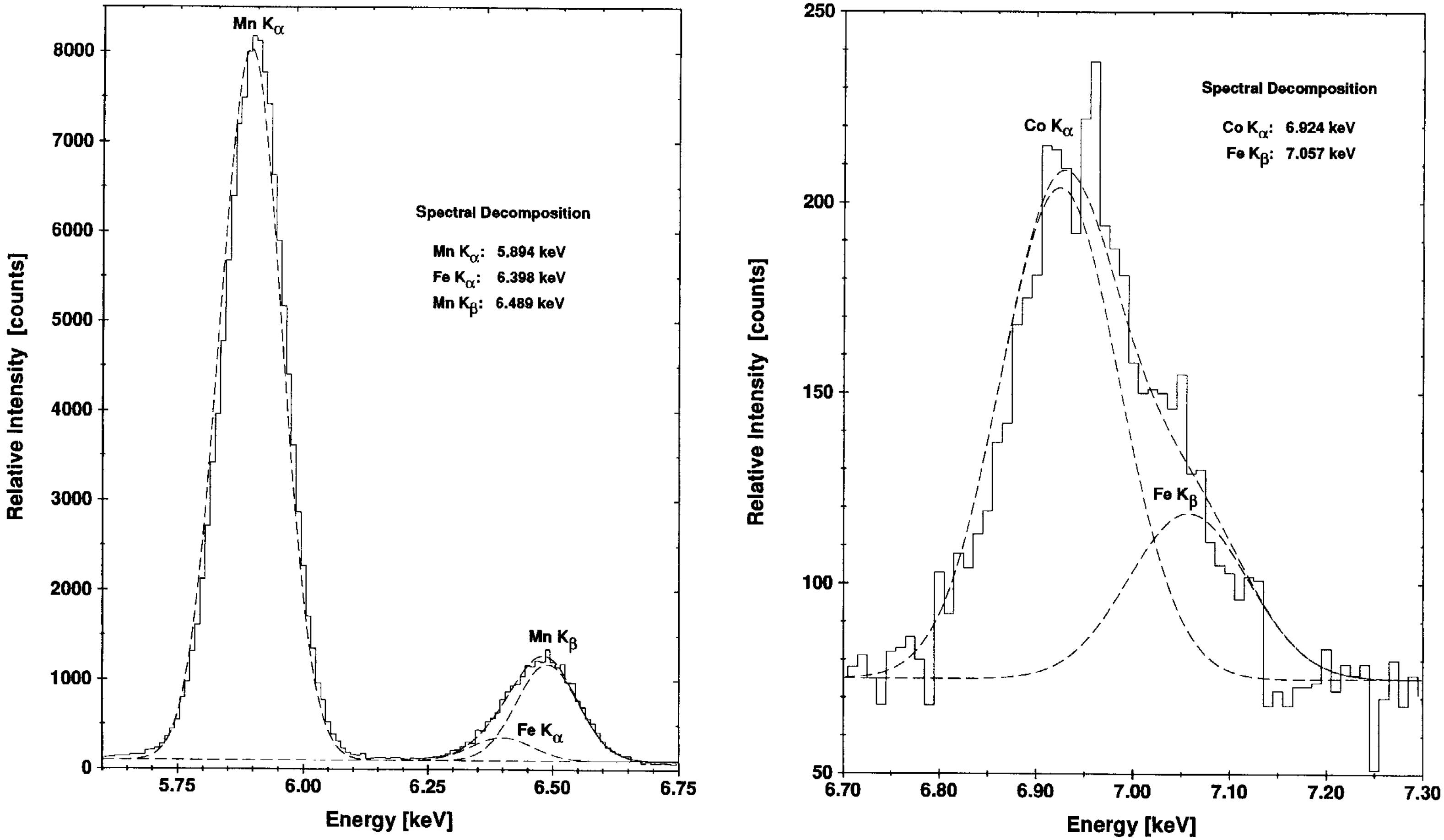

Fig. 6. Spectral deconvolution of the digitized EDS data (Fig. 5b) in the 5.5–7.5 keV region. The peaks for Mn, Fe, and Co were centered on their theoretical energy values, i.e., Mn K_α (5.894 keV), Fe K_α (6.398 keV), Mn K_β (6.489 keV), Co K_α (6.924 keV), and Fe K_β (7.057 keV). The width of the peaks (145 eV) is constant for all the elements, only the peak heights were adjusted. The respective heights in relative intensity units are: Mn K_α = 7940; Fe K_α = 260; Mn K_β = 1080; Co K_α = 129; and Fe K_β = 43.5.

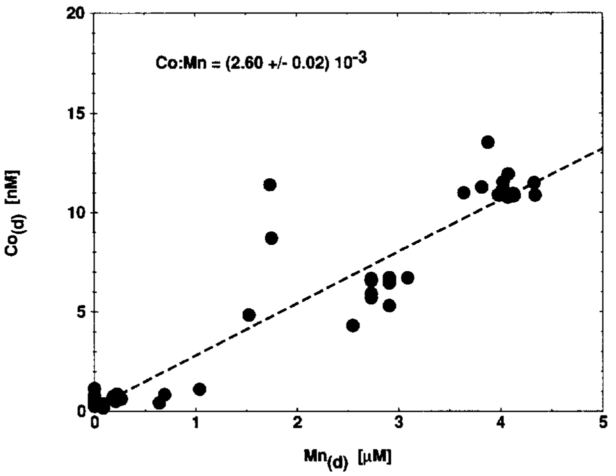

Fig. 7. Dissolved Co:Mn relationship as determined from the water column data of May 1994 and July–August 1995 (ρ = 0.946, n = 51).

Lake, a dimitic lake in the Massif-Central (F), Viollier (1995) reports Co:Mn ratios of 6.3 × 10^{-4} and 8.2 × 10^{-4} for September 1993 and 1994, respectively. Finally, using the Viollier (1995) data for Lake Pavin, a meromictic crater lake in the Massif-Central, one finds a ratio of (3.13 ± 0.02) 10^{-3}, whereas the Co:Mn ratio in sediment trap material varies from 1.5 × 10^{-3} to 2.8 × 10^{-3}. All these ratios are at least an order of magnitude less than the one we determine from individual particles. Aqueous phase concentrations, then, are not simply the result of the dissolution of manganese oxides bearing Co.

A Fe:Mn association can not be evidenced from the bulk water chemical analysis. Conversely, TEM-EDS proved to be a powerful method for determining the amounts of Fe associated with Mn. One should first notice that the Fe:Mn ratio that we have determined is highly variable from particle to particle. This implies that the mechanisms of Fe incorporation in the manganese oxide are not the same. Iron can be present either as adsorbed Fe^{2+} or as amorphous hydrous Fe-oxides aggregates within the matrix of the manganese oxides. Although EDS spectra cannot discriminate between Fe(II) and Fe(III), two mechanisms can explain the presence of Fe in various proportion in manganese oxides. First, a biological path is possible due to the fact that most types of bacteria that are responsible of the oxidation of Mn are known to oxidize Fe, e.g., *Galionella, Leptothrix spp., Leptothrix discophora,* and *Shewanella putrefaciens* (Gounot, pers. commun.; Ehrlich, 1996). In the case of *Arthrobacter siderocapsulatus,* the bacterium generates H_2O_2, which is in turn degraded by the bacterial catalase using Mn^{2+} (Ghiorse, 1984). It has been shown that Fe^{2+} can replace Mn^{2+} (Dubinina, 1978) in this reaction. This suggests that biological processes could be responsible for the simultaneous presence of Fe and Mn in the oxides analyzed. Second, a chemical path can explain the uneven presence of Fe in manganese oxides by considering the possible catalytic effect of freshly produced $Fe(III)_p$ on the oxidation of Mn^{2+} (Hem, 1978) in oxic waters. Moreover, since manganese oxides and colloidal ferric oxy(hydr)oxides have opposite surface charge around neutral pH, the electrostatic interaction of these particles could result in the formation of mixed phase aggregates. According to the TEM observations, particulate iron is present along the entire water column, and could, therefore, easily mix with manganese oxides. Future studies, that will explore redox processes at the molecular level and consider either chemical or biotic controls, are necessary.

5. CONCLUSIONS

The depth distributions of dissolved Co and Mn observed in Paul Lake (MI) demonstrate that their limnological biogeochemical cycles are coupled, although Fe may also be involved incidentally. The inspection of the particulate material by TEM, and its analysis by HREM equipped with a narrow EDS probe, show that bacteria covered by manganese oxide overgrowth are the most likely candidates for the scavenging of Co in the water column. These data provide the first direct evidence of the presence of Co and one of the few indications of the presence of Fe (Tipping et al., 1984) in bacterial manganese oxides, at the level of individual particles.

Co:Mn ratios, inferred from bulk water analyses, are smaller than those established by analytical electron microscopy of individual particles. This indicates either that manganese oxide overgrowths, formed at the surface of bacteria, are enriched in Co compared to the solution, or that Co is bio-accumulated by manganese oxidizing micro-organisms. Moreover, we have shown that these particles can contain a relatively high fraction of Fe, a result which can not be deducted from the change in the chemical composition of the waters.

The TEM-EDS inspection of particles proves to be a powerful tool to study chemical associations in aquatic systems. Used in combination with careful trace element analysis, it opens a completely new horizon for studying the interactions of trace elements with authigenic hydrous oxides formed at oxic/anoxic transitions.

Acknowledgments—This research was supported by the Swiss National Science Foundation (project # 20-42250.94; D.P. and J-F. G.), the National Science Foundation (BCS 93-09349, J-F. G.), and the Agassiz Fund (D. P.). We would like to thank M. Berg (Assistant Director) and R. Hellenthal (Director) for providing us with all the facilities to conduct this research at UNDERC. S. Silliman (University of Notre Dame) kindly supplied the portable CTD-pH-O_2 probe used to perform water column profiles. We are thankful to P. Stadelmann (CIME, EPFL, Lausanne), L. Perring (University of Lausanne), and T. Kozel (University of Notre Dame) for their expertise and guidance in electron microscopy. We are grateful to Dr. W. Davison and two other anonymous reviewers for their suggestions to improve the manuscript.

Editorial handling: L. S. Balistrieri

REFERENCES

Balistrieri L. S., Murray J. W., and Paul B. (1992a) The cycling of iron and manganese in the water column of Lake Sammamish, Washington. *Limnol. Oceanogr.* **37,** 510–528.

Balistrieri L. S., Murray J. W., and Paul B. (1992b) The biogeochemical cycling of trace metals in the water column of Lake Sammamish, Washington: Response to seasonally anoxic conditions. *Limnol. Oceanogr.* **37,** 529–548.

Balistrieri L. S., Murray J. W., and Paul B. (1994) The geochemical cycling of trace elements in a biogenic meromictic lake. *Geochim. Cosmochim. Acta* **58,** 3993–4008.

Boulègue J., Ciabrini J-P., Fouillac C., Michard G., and Ouzounian

G. (1979) Field titrations of dissolved sulfur species in anoxic environments. Geochemistry of Puzzichello Waters (Corsica, France). *Chem. Geol.* **25,** 19–29.

Buffle J., Perret D., and Newman M. (1992) The use of filtration and ultrafiltration for size fractionation of aquatic particles, colloids, and macromolecules. In *Environmental Particles, Volume 1* (ed. J. Buffle and H. P. van Leeuwen), pp. 171–230. Lewis.

Burdige D. J. and Nealson K. H. (1986) Chemical and microbiological studies of sulfide-mediated manganese reduction. *Geomicrobiol. J.* **4,** 361–387.

Carpenter S. R. and Kitchell J. F. (1993) Experimental lakes, manipulations, and measurements. In *The Trophic Cascade in Lakes* (ed. S. R. Carpenter and J. F. Kitchell), pp. 15–25. Cambridge Univ. Press.

Chapnick S., Moore W. S., and Nealson K. H. (1982). Microbially mediated manganese oxidation in a freshwater lake. *Limnol. Oceanogr.* **17,** 1004–1014.

Crowther D. L., Dillard J. D., and Murray J. W. (1983) The mechanism of Co(II) oxidation on synthetic bimessite. *Geochim. Cosmochim. Acta* **47,** 1399–1403.

DeVitre R. R., Buffle J., Perret D., and Baudat R. (1988) A study of iron and manganese transformations at the $O_2/S(\text{-II})$ transition layer in a eutrophic lake (lake Bret, Switzerland): A multimethod approach. *Geochim. Cosmochim. Acta* **52,** 1601–1613.

Diem D. and Stumm W. (1984) Is dissolved Mn^{2+} being oxidized by O_2 in absence of Mn-bacteria or surface catalysts? *Geochim. Cosmochim. Acta* **48,** 1571–1573.

Dubinina G. A. (1978) Mechanism of the oxidation of divalent iron and manganese by iron bacteria growing at neutral pH of the medium. *Mikrobiologiya* **47,** 471–478.

Dyrssen D. and Kremling K. (1990) Increasing hydrogen sulfide concentration and trace metal behavior in the anoxic Baltic waters. *Mar. Chem.* **30,** 193–204.

Dyrssen D. and Wedborg M. (1986) Titration of sulphides and thiols in natural waters. *Anal. Chim. Acta* **180,** 473–479.

Ehrlich H. L. (1996) *Geomicrobiology.* Marcel Dekker Inc.

Emerson S., Kalborn S., Jacobs L., Tebo B. M., Nealson K. H., and Rosson R. A. (1982) Environmental oxidation of manganese(II): Bacterial catalysis. *Geochim. Cosmochim. Acta* **46,** 1073–1079.

Fergusson J. E. (1990) *The Heavy Elements: Chemistry, Environmental Impact, and Health Effects.* Pergamon Press.

Forstner U. and Wittmann G. T. W. (1979) *Metal Pollution in the Aquatic Environment.* Springer Verlag.

Fukai R. (1968) A spectrophotometric method for determination of cobalt in seawater after enrichment with solid manganese dioxide. *J. Oceanogr. Soc. Japan* **24,** 1–9.

Ghiorse W. C. (1984) Biology of iron and manganese depositing bacteria. *Ann. Rev. Microbiol.* **38,** 515–550.

Godart C., Latroche M., Fretigny C., and Levy-Clément C. (1992) EXAFS studies of synthetic γ-MnO_2 and related pyrolusite and ramsdellite minerals. *Phys. Stat. Sol. (a),* **132,** 253–268.

Gregory E. and Staley T. J. (1982) Widespread distribution of ability to oxidize manganese among freshwater bacteria. *Appl. Environ. Microbiol.* **44,** 2435–2446.

Hem J. D. (1978) Redox processes at surfaces of manganese oxide and their effects on aqueous metal ions. *Chem. Geol.* **21,** 199–218.

Honeyman B. D. and Santschi P. H. (1988) Metals in aquatic systems. *Environ. Sci. Technol.* **22,** 862–871.

Honeyman B. D. and Santschi P. H. (1992) The role of particles and colloids in the transport of radionuclides and trace metals in the oceans. In *Environmental Particles, Volume 1* (ed. J. Buffle and H. P. van Leeuwen), pp. 379–423. Lewis.

Lee Y. and Tebo B. M. (1994) Cobalt(II) oxidation by the marine manganese(II) oxidizing *Bacillus sp.* Strain SG-1. *Appl. Environ. Microbiol.* **60,** 2949–2957.

Leppard G. G. (1992) Evaluation of electron microscope techniques for the description of aquatic colloids. In *Environmental Particles, Volume 1* (ed. J. Buffle and H. P. van Leeuwen), pp. 231–289. Lewis.

Manceau A., Gorshkov A. I., and Drits V. A. (1992) Structural chemistry of Mn, Fe, Co, and Ni in manganese hydrous oxides: Part II. Information from EXAFS spectroscopy and electron and X-ray diffraction. *Amer. Mineral.* **77,** 1144–1157.

Mandernack K. W., Post J., and Tebo B. M. (1995) Manganese mineral formation by bacterial spores of the marine Bacillus, strain SG-1: Evidence for the direct oxidation of Mn(II) to Mn(IV). *Geochim. Cosmochim. Acta* **59,** 4393–4408.

Michard G., Viollier E., Jézéquel D., and Sarazin G. (1994) Geochemical study of a crater lake. The Pavin Lake, France: Identification, location, and quantification of the chemical reactions in the lake. *Chem. Geol.* **115,** 103–115.

Murray J. W. (1975) The interaction of cobalt with hydrous manganese dioxide. *Geochim. Cosmochim. Acta* **39,** 635–647.

Nealson K. H., Tebo B. M., and Rosson R. A. (1988) Occurrence and mechanisms of microbial oxidation of manganese. *Adv. Appl. Microbiol.* **33,** 279–318.

Parkhurst D. L. (1995) User's guide to PHREEQC—A computer program for speciation, reaction-path, advective-transport, and inverse geochemical calculations. U.S. Geological Survey Water-Resource Investigations Report 95-4227.

Perret D., Leppard G. G., Müller M., Belzile N., DeVitre R., and Buffle J. (1991) Electron microscopy of aquatic colloids: Nonperturbing preparation of specimens in the field. *Water Res.* **25,** 1333–1343.

Reed S. J. B. (1993) *Electron Microprobe Analysis.* 2nd ed. Cambridge.

Richardson L. L., Aguilar C., and Nealson K. H. (1988) Manganese oxidation in pH and O_2 micro-environments produced by phytoplankton. *Limnol. Oceanogr.* **33,** 352–363.

Schrauzer G. N. (1991) Cobalt. In *Metals and Their Compounds in the Environment: Occurrence, Analysis, and Biological Relevance* (ed. E. Merian), pp. 879–892. VCH.

Schmidt W-D. (1979) Morphologie und Physiologie Manganoxidierender Mikroorganismen-Kultur- und in situ Untersuchungen zur Oekologisch-Mikrobiologischen Characterisierungen von *Metallogenium sp.* und *Siderocapsae geminata* im Plussee. Ph.D. Thesis, Kiel Univ.

Siffert C. (1989) L'effet de la lumière sur la dissolution des oxydes de Fer(III) dans les milieux aqueux. Thèse de Doctorat, ETH.

Spencer D. W., Brewer P. G., and Sachs P. L. (1972) Aspects of the distribution and trace element composition of suspended matter in the Black Sea. *Geochim. Cosmochim. Acta* **36,** 71–86.

St. Amand A. (1990) Mechanisms controlling metalimnetic communities and the importance of metalimnetic phytoplankton to whole lake primary productivity. Ph.D. thesis, Univ. Notre Dame.

Stookey L. L. (1970) Ferrozine: A new spectrophotometric reagent for iron. *Anal. Chem.* **42,** 779–781.

Stumm W. (1992) *Chemistry of the Solid-Water Interface. Processes at the Mineral-Water and Particle-Water Interface in Natural Systems.* Wiley.

Stumm W. (1993) Aquatic colloids are chemical reactants: Surface structure and reactivity. *Colloids Surfaces A* **73,** 1–18.

Tebo B. M. (1991) Manganese(II) oxidation in the suboxic zone of the Black Sea. *Deep-Sea Res.* **38,** 883–905.

Tebo B. M., Nealson K. H., Emerson S., and Jacobs L. (1984) Microbial mediation of Mn(II) and Co(II) precipitation at the O_2/H_2S interfaces in two anoxic fjords. *Limnol. Oceanogr.* **29,** 1247–1258.

Tipping E., Thompson D. W., and Davison W. (1984) Oxidation products of Mn(II) in lake waters. *Chem. Geol.* **44,** 359–383.

Tipping E., Jones J. G., and Woof C. (1985) Lacustrine manganese oxides: Mn oxidation states and relationships to Mn depositing bacteria. *Arch. Hydrobiol.* **105,** 161–175.

U.S. Department of Energy (1994). *Subsurface Science Program: Program Overview.* U.S. DOE.

Viollier E., Albéric P., Jézéquel D., Michard G., Pèpe M., and Sarazin G. (1995) Geochemical study of a crater lake: The Pavin lake, France: Trace elements behaviour in the monimolimnion. *Chem. Geol.* **125,** 61–72.

Viollier E. (1995) Géochimie des éléments traces en milieu lacustre. Thèse de Docteur d'Universié, Univ. Denis Diderot.

Whitfield M. and Turner D. R. (1987) The role of particles in regulating the composition of natural waters. In *Aquatic Surface Chemistry* (ed. W. Stumm), pp. 457–493. Wiley.

Williams D. R. (1971) *The Metals of Life. The Solution Chemistry of Metal Ions in Biological Systems.* Van Nostrand Reinhold Co.